Investigation of a Specific Magnetic Characterization dedicated to Manufactured Massive Cores

[1,2]M. Borsenberger, [2]A. Benabou, [1]C. Baudouin, [1]R. Bigot, [3]P. Faverolle, [3]J.-C. Mipo

[1]LCFC, ENSAM Campus de Metz, 4 Rue Augustin Fresnel, 57078 Metz Cedex 3, France
[2]L2EP, Université des Sciences et des Technologies de Lille, 59655 Villeneuve d'Ascq, France
[3]Valeo Powertrain Systems, 2 Rue André Charles Boulle, 94046 Créteil Cedex, France
E-mail: marc.borsenberger@ensam.eu

Abstract— **Magnetic parts are usually composed of a stack of electrical steel laminations to reduce the eddy current losses. However, for cost reasons or for specific applications the magnetic core can be made from massive steel and thus manufactured with adapted processes such as forging. This kind of process may imply anisotropy and severe inhomogeneity of the material properties. Therefore, for accurate design or study of the electromagnetic part, it is necessary to account for the real properties of the material. In that context, most of the standard characterization procedures are not adapted to represent the magnetic flux behavior through a bulk material and applicable for material anisotropy at the same time. The proposed specific characterization procedure aims at considering these both aspects.**

Index Terms—**FE-Simulation, Magnetic characterization, Massive sampling, Material properties.**

I. INTRODUCTION

Usually, in electrical machines, the magnetic core is made from stacked laminations in order to limit the eddy current losses and improve the efficiency of the energy conversion. Nevertheless, for special electrical machines, due to cost reasons in mass production, massive magnetic parts such as the rotor can be incorporated. Moreover, with massive magnetic parts, the magnetic flux can be three-dimensional, allowing specific designs of electrical machines. Then, as their performances are strongly related to the magnetic properties of the employed materials, the use of massive magnetic parts requires to pay special attention to the bulk properties of the material. In practice, when designing such electrical devices, numerical tools, such as the finite elements analysis, are usually employed. The material magnetic properties implemented in these tools may not correspond to the real behavior as they are mostly considered as homogeneous and consequently the performances of the simulated electrical device may be different from the experimental one. Therefore, for a more accurate study and/or design of the device, the characterization of the magnetic behavior, by considering the influence of the manufacturing processes, is necessary.

Regarding the massive magnetic parts, they are usually manufactured with a succession of operations including hot forging which impact on the magnetic permeability has been illustrated by Ghodsi [1]. However, the scientific literature content is mostly dedicated to the study of laminated electrical steels and the related manufacturing processes. For example, the rolling process impact in terms of rolling direction and plastic strain on the magnetic properties has been studied by Landgraf [2] or Chun-Kan [3]. Also, different cutting processes (shearing, laser and wire electric discharge machining) have been compared by Kurosaki [4] in terms of specific losses and magnetizing force to reach 1.5T. In all these works, phenomenological approaches are adopted and the results may be extended with difficulty to other applications or for numerical modelling.

Another approach consists in considering the inherent material properties, such as the microstructure, mechanical stress or plastic strain, in order to understand the related magnetic properties. In the literature, a correlation between grain size and specific core losses has been revealed in several works [5][6][7]. Regarding the iron losses, an optimum grain size exists for a given material at a given operating frequency because of the antagonist effects of eddy currents and hysteresis losses. Other studies focus on the effect of mechanical stress and plastic strain on magnetic properties [8][9][10]. They demonstrate experimentally that slight tensile stresses (for non-pre-stressed laminations) can improve the magnetic properties whereas compression stresses and severe tensile stress deteriorate the magnetic properties. Furthermore, plastic strain, in cold deformation, results in a general flattening of the hysteresis loop and consequently in a deterioration of the magnetic properties.

These observations have largely been made in case of laminated steels because of their large use in magnetic core applications. Moreover, magnetic characterizations are most of the time performed on laminations with techniques such as those described by the IEC 60404 standard [11] (Epstein or Single Sheet Tester). Other non-destructive techniques have also been proposed [12], but remain limited in terms of magnetization level. For massive magnetic parts, a first approach is the extraction of ring-shaped samples, which is not always convenient due to small geometric dimensions available in the initial part and also because this technique does not allow the consideration of anisotropic properties.

Therefore, a specific characterization procedure is proposed in this work. The proposed approach consists in extracting parallelepipedic samples, which are relatively massive samples to avoid potential mechanical stress relieving. Then, the characterization is performed while the magnetic flux goes though the bulk material with limited edge or surface effect of material properties. This kind of geometry allows also to consider different directions of sampling within the main part to take into account mechanical and material anisotropies.

First, the experimental device is described, along with its numerical study to verify the feasibility and the relevance of the measurement setup. Then, the

measurement validation is performed on the basis of a sensitivity and repeatability analysis together with a reference measure. Finally, measurements are performed on selected samples, with different mechanical and material anisotropies, to reveal the impact on the magnetic properties.

II. DESCRIPTION OF THE EXPERIMENTAL DEVICE

A. General description

The sample is placed between the magnetic poles of an electromagnet device (Figure 1) that generates the excitation field at low-frequency. The extreme surfaces of the parallelepipedic sample must be as parallel and as flat as possible to limit the parasite air gaps which would increase the leakage flux around the sample and introduce a strong gradient of the magnetic field H between the poles of the electromagnet device.

As a preliminary development, the input current is controlled to be sinusoidal. Note that, in the quasi-static conditions, the hysteresis behavior is only dependent on the extreme values of the magnetic field and not on its waveform. In our case, a controlled current source is connected to the input of the electromagnet device. The frequency must remain low (< 0.5Hz) because of the design of the electromagnet and also to avoid skin effects in the sample.
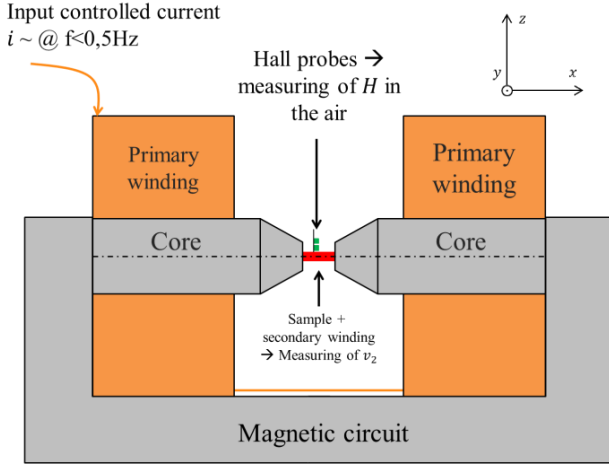

Figure 1: Schematic of the characterization equipment

First, to measure the polarization J of the sample, a secondary coil is placed on a plastic support in which the sample can be inserted. This way, the eventual dispersion in measurements, due to different windings placed directly on the different samples, is limited. The electromotive force v_2 is measured with a voltage probe. From this measure the magnetic polarization of the sample J is determined with the compensation of the flux in the air:

$$J = \frac{1}{S_{sample}} \left(\frac{1}{n_2} \int v_2(t)dt \; - \mu_0 H \, S_{winding} \right) \qquad (1)$$

where S_{sample} is the cross section of the sample, n_2 and $S_{winding}$ are respectively the number of turns and the cross-section of the secondary winding, μ_0 the magnetic permeability of the void and H the magnetic field estimated in the sample.

To measure the magnetic field H, two Hall probes are placed above the sample. They deliver a voltage proportional to the magnetic field H at two known locations in the air around the sample. As a first approach, a linear extrapolation is chosen to estimate the magnetic field at the surface of the sample:

$$H = \frac{H_{probe\,1} z_{probe\,2} - H_{probe\,2} z_{probe\,1}}{z_{probe\,2} - z_{probe\,1}} \qquad (2)$$

where $H_{probe\,i}$ and $z_{probe\,i}$ are respectively the magnetic field measured by the probe i and its distance to the sample surface.

Generally, the electromagnetic numerical tools require the use of a single-valued behavior law of the materials. Therefore, from the measured hysteresis loops, the normal polarization curve will be extracted. This curve is drawn from the maximum magnetic fields and polarizations of centered minor loops measured at different levels of polarization, as illustrated in Figure 2.
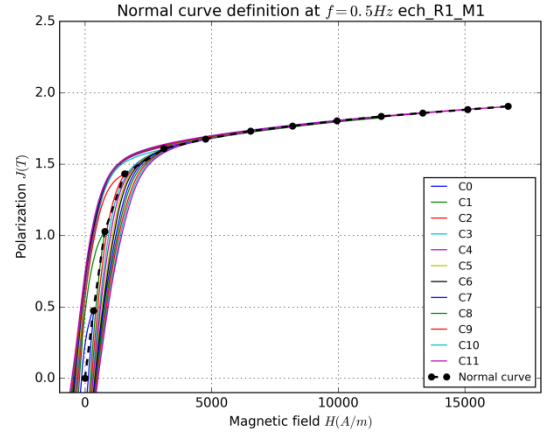

Figure 2: Normal curve extraction from centered loops

In addition, the specific core losses are determined in our case for a given applied magnetic field H:

$$\mathcal{P}_{H[kA/m]}[W/kg] = \frac{f}{\rho} \int H dB \qquad (3)$$

where f is the frequency in Hz, ρ the material density in kg/m^3 and B the magnetic flux density in T.

B. Numerical study of the device

To validate the principle of the presented experimental setup, a numerical model of the measurement technique has been developed. The three dimensional electromagnetic problem is solved thanks to a time stepping finite element (FE) method and using electric potential formulation to consider the electrical conductivity in the sample. The magnetic behavior law of the sample used in the model is similar to what is expected for the considered material.

From this model, an investigation on several hypotheses can be performed in order to improve the understanding of the different sources of errors. The first hypothesis considers that the magnetic field H and the magnetic flux Φ are measured at the same position. In fact, the Hall probes measure the magnetic field at two points in the space surrounding the sample and along a given direction, whereas the secondary winding gives the global magnetic flux density which passes through the

surface of the winding and on a given length of the winding. The equation (1) also supposes that the magnetic field in the sample and in the air gap between the winding and the sample is the same.

The numerical simulation shows that the magnetic field surrounding the sample is not homogeneous. In Figure 3, the distribution of the magnetic field is shown in a cross-section located in the middle of the sample between the electromagnet poles.
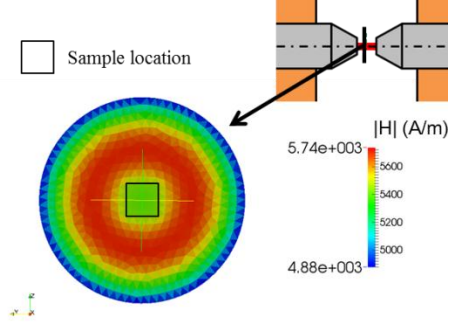

Figure 3: Distribution of the magnetic field H between the poles of the electromagnet according to the FE simulation

The homogeneous center of this distribution ($\approx$ 5300 A/m) represents the sample. Then, by increasing the distance to the sample, the magnetic field increases to a maximum and decreases.

This calculated magnetic field profile is verified experimentally by moving the Hall probes along the Z-axis (back to Figure 1). The results are shown in Figure 4, where the left axis represents the outer radius of the winding and the vertical dashed line the limit of the flat surface of the poles.
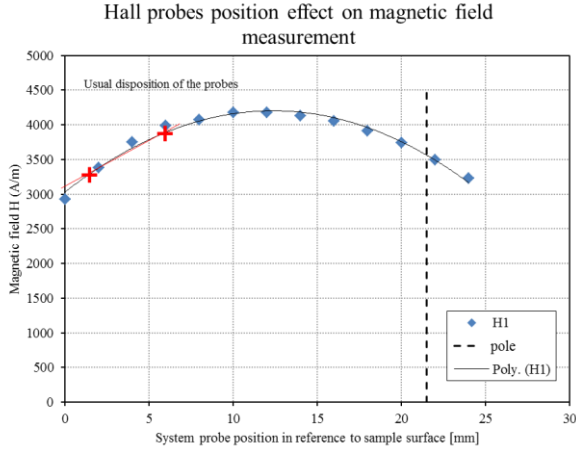

Figure 4: Magnetic field distribution above the sample (experimental)

The linear extrapolation from equation (2) is made from the two positions of the Hall probes represented by the two red points in Figure 4, and gives in that case a relative error of 1.32%.

Furthermore, another assumption is a uniform distribution of the magnetic flux density in the sample in every cross section along the length of the secondary winding which is confirmed by the simulation.

III. VALIDATION

A. Sensitivity and repeatability

To validate the characterization protocol, two steps are performed: a qualitative validation and comparison to a reference measure.

The qualitative validation is represented by the ability of the characterization protocol to give always the same result (precision according Standard ISO 5725-1). The major source of errors is related to the relative positions of the sample, the electromagnet device, the probes and the secondary winding. A preliminary experimental sensitivity analysis has been performed. The effect of the following parameters has been investigated:

- The Hall probes position regarding the sample: along X, Y and Z-axis (Figure 1),
- The secondary winding position: centered or in contact with a pole (along X direction),
- The sample position in the magnetic poles

It has been observed that the secondary winding position has a minor impact on the measures whereas the relative position of the Hall probes, sample and electromagnet poles must be accurate. Indeed the Hall probes must be as close to the sample as possible in order to limit the error due to the linear extrapolation to estimate the magnetic field at the sample surface.

To go further in the qualitative validation, a set of ten measurements are performed on the same sample under repeatability conditions. The following protocol is applied for each measurement:

- Positioning the sample between the magnetic poles,
- Compensating the remnant induction in the magnetic circuit for a given amplitude of the excitation field,
- Recording the monitored quantities for ten different levels of the input current,
- Post-processing of the measures.

The results associated to the normal curves are shown in Figure 5 and those associated to the losses, at an excitation field of 16kA/m, in Figure 6.
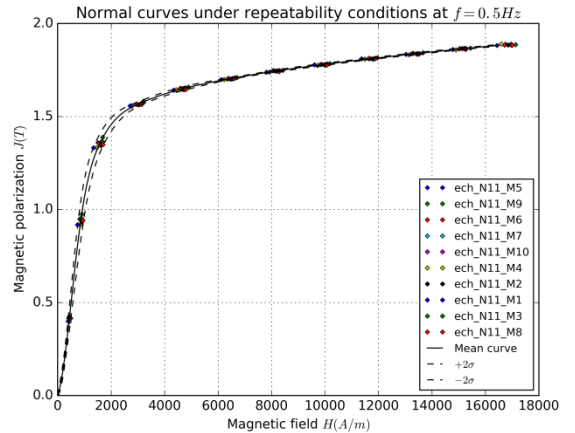

Figure 5: Normal curves under repeatability conditions for the considered test sample

Qualitatively the Figure 5 shows slight variations on the normal curves. Considering the $\pm 2\sigma$ interval, where σ is the standard deviation, the variations in the result is mostly due to the uncertainty on the measure of the magnetic field H. For example, to compare numerically the normal curves, and as a first approach, the chosen criterion is the required magnetic field $H_{1.5}$ to reach a magnetic polarization of 1.5T. Considering a cubic interpolation between the measured points, the repeatability of the measurement can be qualified with an average value of

$\overline{H}_{1.5}$=2320 A/m and a standard deviation of σ=115 A/m, representing a coefficient of variation σ/$\overline{H}$ =4.8%. Concerning the specific losses at 16kA/m shown in Figure 6, the coefficient of variation σ/$\overline{\mathcal{P}}$ represents 2.13%.
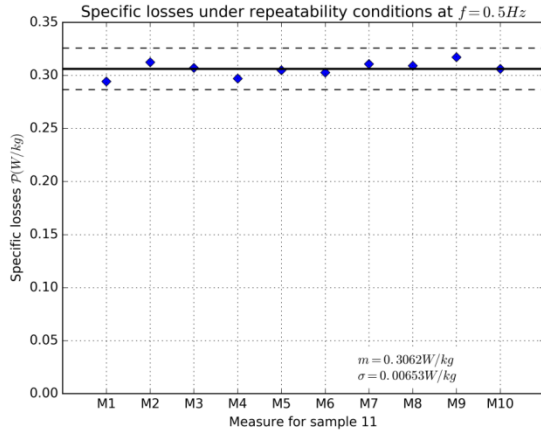

Figure 6: Specific losses under repeatability conditions for the considered test sample

Note that, to distinguish the effect of material parameters on the magnetic properties, the calculated error of precision must be significantly inferior to the variations observed on samples with different magnetic properties.

B. Comparison to a reference measurement

The precision of the measure has been investigated in the previous section. The next parameter to be considered to validate the accuracy of the characterization device is the trueness (according Standard ISO 5725-1). This parameter describes the deviation between the measured and the true value. To do this, measurements are performed on reference samples from the same cylindrical hot rolled bar. The material anisotropies and eventual variations in the material properties, due to hot rolling and impact of the sampling technique, must be taken into account. These samples are obtained using wire electric discharge machining, assumed to have a repeatable and limited impact on the magnetic properties [4]. The characterization is performed on parallelepipedic samples extracted from a hot rolled cylindrical bar billet. The experimental results are compared to measurements obtained from the standard ring core technique and from the same bar. In this kind of billet, mechanical anisotropy is often qualified with the fiber orientation, that is to say the elongation of the malleable inclusions in the matter in the same direction as the flow of matter during the forming process [13]. Hence the reference samples are taken in a way, described in Figure 7, that the magnetic flux has a similar trajectory orientation regarding the fiber orientation in the billet. Also, the locations of the samples and the ring core are chosen at a similar radius in order to limit the impact of an eventual variation of the material properties (such as the microstructure) along the radius.
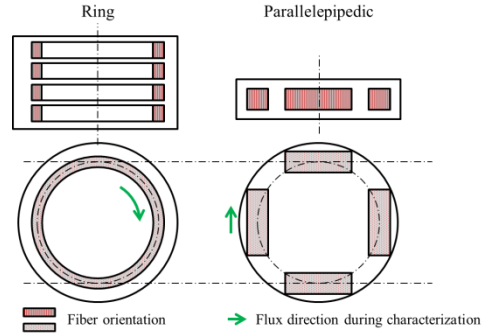

Figure 7: Reference sample, flux direction and fiber orientation

The experimental protocol consists in repeating three times the measurements for each sample at 12 levels of the input current. The normal curves obtained for the samples are shown in Figure 8 where R_i stands for the sample number and M_i for the measure repetition.
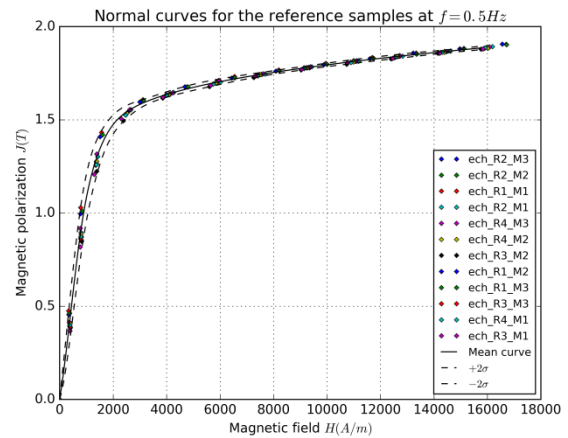

Figure 8: Normal curves for reference samples

The magnetic field needed to reach a polarization level of 1.5T has an average value of 2190/m and a standard deviation of 142A/m over these twelve measurements, that is to say a coefficient of variation of 6.7%. The average value of the specific losses is 0.248 W/kg and the associated standard deviation is 0.011 W/kg over the twelve measures, representing a coefficient of variation of 4.4%.

This represents slightly more variation than the repeatability measures. The conclusion is that the reference samples are slightly different from each other in terms of specific losses and magnetic field $H_{1.5}$.

The ring core measure has been performed to investigate about the relevancy of the specific characterization. Three ring cores have been extracted from the same bar as the parallelepipedic samples (Figure 7). Each ring core is measured three times. The primary and the secondary windings have been designed to reach a comparable magnetic field range. The magnetic quantities are evaluated according to the following formulas:

$$H = \frac{n_1 i}{l_m} \qquad (4)$$

$$J = \frac{1}{n_2 S} \int v_2(t)dt - \mu_0 H \qquad (5)$$

where n_1 and n_2 are the number of turns of respectively the primary and secondary winding, l_m the characteristic

length of a magnetic core according to Standard IEC 60205. Here the secondary winding cross section is assumed to be the same as the sample cross section. The comparison between the normal curves from specific and standard characterizations is shown in Figure 9.
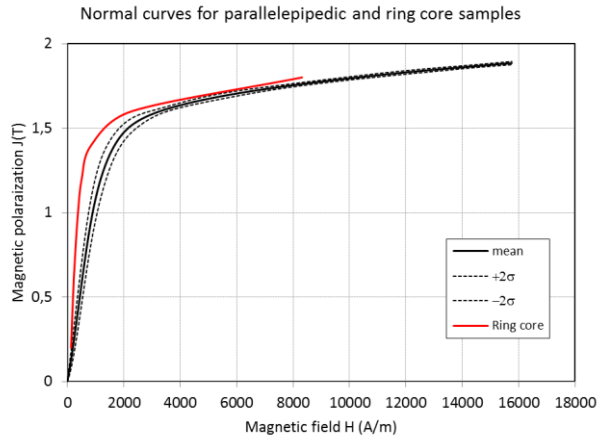

Figure 9: Comparison between the reference samples and the ring core

In the standard measures (ring core), the required field to reach 1.5T is $H_{1.5} = 1425$ A/m. In that case, the specific characterization gives a value about 50% superior. As previously indicated, this error may be imputed to an overestimation of the magnetic field from the Hall probes and the linear extrapolation from a parabolic evolution of the magnetic field in the air.

Even though the measure is still not quantitative, given the precision of the specific characterization, the device is capable of distinguishing the variation of magnetic properties which is satisfying for the goal of the present work.

IV. APPLICATION TO MASSIVE MAGNETIC SAMPLES HAVING DIFFERENT MATERIAL PROPERTIES

As explained in the introduction, the manufacturing process, like hot forging, has a strong impact on material and mechanical properties. The proposed characterization approach is now used to study the impact of these inherent properties on magnetic properties. The sensitivity of the device is illustrated with selected material parameters. On one hand, the grain size influence on magnetic properties, especially the specific losses, is verified and on the other hand, the influence of fiber orientation on the magnetic properties is investigated.

A. Grain size

Three sets of samples are investigated in this section. The first one (set A) is directly sampled in a hot rolled cylindrical bar, the corresponding grain size index is 6 ASTM (45µm). The two other are obtained after different heat treatments. The set B has been obtained with a normalizing heat treatment, at a temperature of 900°C during 10 minutes with air cooling. The obtained grain size index is 9 ASTM (15µm). The set C has been obtained with a grain growth heat treatment, at a temperature of 1100°C during 20 hours and furnace cooling. The obtained grain sized index is about 0 ASTM (350µm). The grain size is evaluated using the intercept segment method according the standard ISO 643. The corresponding micrographies are shown in Figure 10.
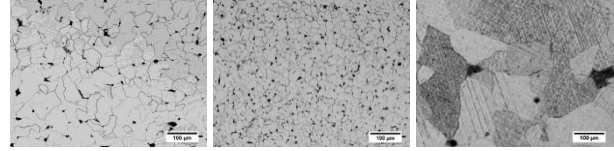

Figure 10: Micrographies for the two different sets of samples
(left: set A; middle: set B; right: set C)

The samples have been magnetically characterized with the proposed technique. The results concerning the magnetic field needed to reach a polarization of 1.5T are shown in table I.

TABLE I
MAGNETIC FIELD $H_{1.5}$ FOR DIFFERENT GRAIN SIZES

Grain size	9 (15 µm)	6 (45 µm)	0 (350 µm)
$\overline{H_{1.5}}$	2350 A/m	2250 A/m	2200 A/m
$\sigma(H_{1.5})$	200 A/m	160 A/m	220A/m

Considering only the mean values, these results may show a trend that the larger the grain is, the lower the magnetic field $H_{1.5}$ is, which describes better magnetic properties. However, the standard deviation of these measures prevents an evident conclusion.
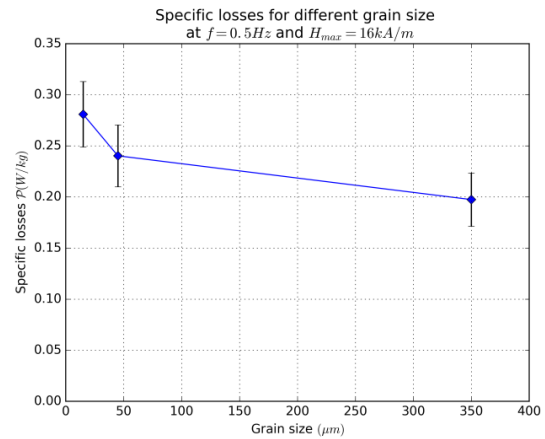

Figure 11: Influence of the grain size on specific losses

Regarding the specific losses, the results in Figure 11 show a clear trend that these losses decrease with larger grains. Considering the given frequency of 0.5Hz, the eddy current losses seems not significant and a diminution of the hysteresis losses with larger grain size is expected as found in the literature [5].

B. Fiber orientation

As discussed in the introduction, the literature shows difference in terms of magnetic properties according to the direction of characterization regarding the rolling direction for electrical steel laminations. The phenomenon is significant between the two cross direction 0° and 90° [2]. In this case, due to the hot rolling process, the fiber is oriented in the same direction as the cylindrical bar axis. To evaluate the impact of the fiber orientation, two sets of samples are taken from the billet according different directions represented in Figure 12.
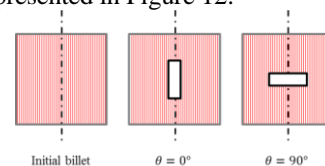

Figure 12: Sampling with different fiber orientations

These samples have been characterized with the presented device at 0.5Hz and the same 12 levels of input

current. The table II shows the specific losses at 16 kA/m for the two sets of investigated samples. The distance between the two sets is not significant regarding the associated standard deviations.

TABLE II
SPECIFIC LOSSES AT 0.5HZ AND 16KA/M FOR DIFFERENT DIRECTIONS

θ	0°	90°
$\overline{\mathcal{P}_{16}}$	0.240 W/kg	0.247 W/kg
$\sigma(\mathcal{P}_{16})$	0.015 W/kg	0.011 W/kg

The Figure 13 shows the mean normal curves for the two sets of samples. For the direction $\theta = 0°$, the magnetic field required to reach 1.5T of polarization is $H_{1.5} = 2250$ A/m with a standard deviation of 160 A/m. Concerning the direction $\theta = 90°$, the respective values are 2190 A/m and 142 A/m.
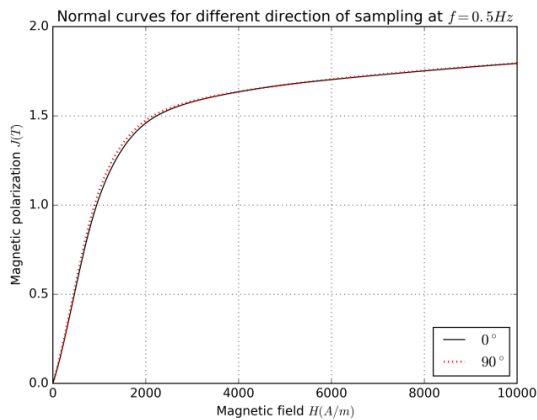

Figure 13: Normal curve for different direction of sampling

The proposed specific protocol allows to verify that, for this steel grade (with a very low content of element of addition) for the frequency of 0.5Hz, fiber orientation has no significant impact on magnetic properties.

V. CONCLUSION

The present work introduces the investigation of a specific magnetic characterization technique to assess the influence of material properties. The literature shows many results in terms of impact of the material properties and processes on magnetic properties for laminated samples. The objective of the proposed approach is to extend all these results to massive samples, and keeping the possibility to investigate material anisotropies.

The presented device rests on a classic method of magnetic flux measurement and magnetic field estimation. The section III.A confirms that the device is able to give repeatable measures. Nevertheless, the difference with the reference measure on ring cores revealed that the magnetic field H is overestimated and the measures are not quantitative yet. Several trays of improvement of the characterization technique can be tested. The addition of more Hall probes to estimate the quadratic profile of the magnetic field within the electromagnet poles can reduce the error due to the linear extrapolation. Modifying the magnetic circuit topology or adding a magnetic shielding can also positively impact the spatial evolution of the magnetic field and make the linear extrapolation relevant.

At the end of this work an application of the device, to study the impact of material properties on magnetic properties, has been proposed. Among the different sets of samples investigated, the standard deviation of the magnetic field $H_{1.5}$ remains slightly superior to the error of repeatability. This confirms certain homogeneity of magnetic respectively material properties between the samples inside a same set. The influence of the material properties on the normal curves and the magnetic field $H_{1.5}$ are not significant for the investigated parameters.

However it has been shown that the grain size has a significant impact on specific losses, which is in accordance with the literature.

The illustration can be extended to other material parameters which are also investigated in the literature, such as crystallographic texture, plastic strain or residual stress. Investigating other steel grades with more element of addition result in more pronounced inclusions and may show differences of magnetic properties according to fiber orientation.

The immediate perspective of the work consists in improving the protocol with the proposed solutions and to apply the methodology to other material parameters in order to establish empiric models to predict their influence on magnetic properties.

REFERENCES

[1] M. Ghodsi and S. M. R. Loghmanian, "Effect of forging on ferromagnetic properties of low-carbon steel," 2011, pp. 1–3.

[2] F. J. G. Landgraf, M. Emura, J. C. Teixeira, and M. F. de Campos, "Effect of grain size, deformation, aging and anisotropy on hysteresis loss of electrical steels," *J. Magn. Magn. Mater.*, vol. 215–216, pp. 97–99, Jun. 2000.

[3] C.-K. Hou and S. Lee, "Effect of rolling strain on the loss separation and permeability of lamination steels," *IEEE Trans. Magn.*, vol. 30, no. 2, pp. 212–216, Mar. 1994.

[4] Y. Kurosaki, H. Mogi, H. Fujii, T. Kubota, and M. Shiozaki, "Importance of punching and workability in non-oriented electrical steel sheets," *J. Magn. Magn. Mater.*, vol. 320, no. 20, pp. 2474–2480, Oct. 2008.

[5] M. F. de Campos, J. C. Teixeira, and F. J. G. Landgraf, "The optimum grain size for minimizing energy losses in iron," *J. Magn. Magn. Mater.*, vol. 301, no. 1, pp. 94–99, Jun. 2006.

[6] R. PremKumar, I. Samajdar, N. N. Viswanathan, V. Singal, and V. Seshadri, "Relative effect(s) of texture and grain size on magnetic properties in a low silicon non-grain oriented electrical steel," *J. Magn. Magn. Mater.*, vol. 264, no. 1, pp. 75–85, Aug. 2003.

[7] E. J. Gutiérrez-Castañeda and A. Salinas-Rodríguez, "Effect of annealing prior to cold rolling on magnetic and mechanical properties of low carbon non-oriented electrical steels," *J. Magn. Magn. Mater.*, vol. 323, no. 20, pp. 2524–2530, Oct. 2011.

[8] V. E. Iordache, E. Hug, and N. Buiron, "Magnetic behaviour versus tensile deformation mechanisms in a non-oriented Fe–(3 wt.%)Si steel," *Mater. Sci. Eng. A*, vol. 359, no. 1–2, pp. 62–74, Oct. 2003.

[9] L. Bernard and L. Daniel, "Effect of Stress on Magnetic Hysteresis Losses in a Switched Reluctance Motor: Application to Stator and Rotor Shrink Fitting," *IEEE Trans. Magn.*, vol. 51, no. 9, pp. 1–13, Sep. 2015.

[10] L. Vandenbossche, S. Jacobs, D. Van Hoecke, and E. Attrazic, "Impact of mechanical stresses on the magnetic performance of non-oriented electrical steels and its relation to electric machine efficiency," in *2015 IEEE Transportation Electrification Conference and Expo (ITEC)*, 2015, pp. 1–6.

[11] IEC, "IEC 60404-2:1996 - Magnetic materials - Part 2: Methods of measurement of the magnetic properties of electrical steel sheet and strip by means of an Epstein frame." 1996.

[12] L. Arbenz, A. Benabou, S. Clénet, J.-C. Mipo, and P. Faverolle, "Characterization of the local incremental permeability of a ferromagnetic plate based on a four needles technique," in *SMM*, 2015.

[13] J. Pokorny and A. Pokorny, "Action du corroyage sur la structure de coulée des aciers," *Tech. l'ingénieur Mise en forme des aciers, Alum. autres métaux alliages*, vol. base docum, no. ref. article : m610, 2015.